J Mater Sci (2007) 42:7191–7197
DOI 10.1007/s10853-007-1571-4

Method for preparing highly dispersed Pt catalysts on mesoporous carbon support

Jianhuang Zeng · Fabing Su · Jim Yang Lee · X. S. Zhao · Jianjun Chen · Xiaohua Jiang

Received: 6 November 2006 / Accepted: 30 January 2007 / Published online: 10 May 2007

Abstract Two Pt catalysts supported on template-synthesized mesoporous carbons (MC) were prepared by the conventional wet-impregnation method (Pt-impreg/MC) and by the less commonly used colloidal deposition method (Pt-coll/MC) to examine the effect of preparation method on catalyst performance. The catalysts were characterized by transmission electron microscopy, field-emission electron microscopy, thermogravimetric analysis and X-ray diffraction. The electro-oxidation of methanol in acidic solutions for direct methanol fuel cells at room temperature was used as the test reaction. CO anodic stripping voltammetry and cyclic voltammetry both recorded enhanced performance for Pt-coll/MC relative to Pt-impreg/MC. The poorer application performance of Pt-impreg/MC can be attributed to the transport resistance in the mesopores, and to the entrapment of a sizable fraction (40%) of Pt nanoparticles in the mesopores which are not readily accessible to the reactants under the reaction conditions.

J. Zeng (✉) · J. Chen · X. Jiang
Room C711, Research Institute of Tsinghua University in Shenzhen, Shenzhen High-Tech Industrial Park, Shenzhen 518057, China
e-mail: JHZeng@gmail.com

F. Su · J. Y. Lee · X. S. Zhao
Department of Chemical and Biomolecular Engineering, National University of Singapore, 10 Kent Ridge Crescent, Singapore 119260, Singapore

Introduction

The current renewed interest in the synthesis of carbon materials is driven by the projected benefits of nanostructured carbons in advanced applications such as hydrogen storage, electrochemical supercapacitors and catalyst supports [1–4]. Porous carbons with well defined nanostructures are being pursued as catalyst supports because their high surface areas and structural regularity are potentially useful features for the dispersion of catalytic metal nanoparticles. Porosity in carbon is generated by three types of pores. The largest contribution comes from the micropores (<2 nm), followed by the mesopores (2–50 nm) and the macropores (>50 nm). While the pores in carbon can contribute to a high surface area, the transport of reactants and products (particularly in the liquid state) through them is difficult when the pores are smaller than 10 nm. However, micropores are ubiquitously present in most of carbon black catalyst supports in use today.

The dispersion of catalytic metal on carbon is often based on the wet impregnation technique. In this method the metal precursor salt is mixed with a carbon slurry, followed by the addition of a chemical reducing agent [1, 2, 5, 6]. The dissolved metal ions, e.g. $PtCl_6^{2-}$ and/or Ru^{3+}, while small enough to penetrate the micropores in carbon, are often preferentially reduced at the pore mouths [7, 8]. We have previously demonstrated that wet-impregnated Pt catalysts supported on microporous carbon with a graphitic shell could outperform those supported on microporous carbon without the graphitic shell in the room temperature electrooxidation of methanol [9]. This is because the graphitic carbon shell conceals most of the micropore openings, therefore preventing the deposition of catalytic metal in deep recesses of the pores which are less accessible to the reactants. A less often used catalyst preparation method

may also be used: the adsorption of a suitably prepared colloidal metal solution on carbon [10]. The preformed metal nanoparticles could deposit only on the carbon exterior surface if they are made bigger than the pore openings in the carbon, and no entrapment of the catalytic metal to undermine metal utilization would occur. To prove this we have compared the performance of two series of Pt catalysts supported a specifically designed, ordered mesoporous carbon with an average pore size smaller than that of the depositing colloidal Pt particles. One of them was prepared by the conventional wet-impregnation method while the other was based on the deposition of colloidal Pt particles with size larger than the pores in the mesoprous carbon. Catalyst performance in areas such as mass activity and CO tolerance in room temperature methanol oxidation reaction was measured. The results clearly show that the colloidal approach is a better method for preparing electrocatalysts on mesoporous carbon.

Experiments

Chloroplatinic acid (H_2PtCl_6) from Aldrich, sodium borohydride ($NaBH_4$), sodium citrate, sulfuric acid (95–97%), benzene, hydrofluoric solution (48%), ethanol and methanol from Merck were used as received without further purification. Filtered de-ionized water was used throughout the study.

Synthesis of mesoporous carbon (MC)

The synthesis of mesoporous carbon was based on a previous publication, using the chemical vapor deposition of benzene [6]. Briefly, about 0.5 g of pure silica SBA-15 template was heated at the rate of 5°C min^{-1} to 900 °C in high purity N_2 (30 cm^3 min^{-1}) in a quartz tube. The gas was then switched to 10 wt.% benzene vapor in N_2 (30 cm^3 min^{-1}) and heating continued at 900 °C for another hour. The carbon-coated template was then cooled down to room temperature in N_2 and etched with a 46% HF solution to remove the template, followed by copious washing with de-ionized water. Mesoporous carbon (MC) was recovered by filtration, and air-dried at 150 °C for 5 h.

Preparation of mesoporous carbon supported Pt catalysts

Pt-coll/MC (Pt supported on MC by colloidal deposition): 2 mL 50 mM H_2PtCl_6 and 4 mL 50 mM sodium citrate were mixed with 120 mL de-ionized water in a conical flask. 2 mL 0.5 M $NaBH_4$ was added dropwise under vigorous stirring at room temperature. $NaBH_4$ was used in excess (2.5 times the stoichiometry for the complete reduction of Pt^{4+} to the elemental state [11]). Stirring continued for 6 h before 78 mg carbon was added to the Pt sol. The mixture was then ultra-sonicated for 1 h followed by overnight stirring to allow for the equilibrium adsorption of Pt sol on MC. The solid phase was recovered by filtration, and washed copiously with water. The recovered solid was then dried in vacuum at 40 °C overnight.

Pt-impreg/MC (Pt supported on MC by the wet impregnation method): 2 mL 50 mM H_2PtCl_6 and 4 mL 50 mM sodium citrate were mixed with 120 mL de-ionized water containing 78 mg of carbon. After 30 min of sonication, 2 mL 0.5 M of $NaBH_4$ was introduced dropwise to the carbon suspension with vigorous stirring at room temperature. The rest of the preparation procedures followed the same as those in the preparation of Pt-coll/MC.

Materials characterizations

The pore characteristics of MC was investigated by physical adsorption of nitrogen at the liquid-nitrogen temperature (–196 °C) on an automatic volumetric sorption analyzer (Quantachrome, NOVA1200). Prior to the measurements, the sample was degassed at 200°C for 5 h in vacuum. Specific surface area was determined by the Brunauer–Emmett–Teller (BET) method using relative pressures in the range of 0.05–0.2. The total pore volume was obtained from the volume of nitrogen adsorbed at a relative pressure of 0.99. The pore size distribution (PSD) curve was derived from the adsorption branch by the Barrett–Joyner–Halenda (BJH) method. Pore size was estimated from the maximum in the BJH-PSD curve. X-ray powder diffraction (XRD) patterns of the catalysts were recorded by a Rigaku D/Max-3B diffractometer (Shimadzu), using CuK_α radiation (λ = 1.5406 Å). The diffraction data was curve fitted by least square using a program provided by the equipment manufacturer. The Pt loadings in the catalysts were determined by thermogravimetric analysis (TGA), using a Thermal Analysis Instruments 2050 analyzer and an air flow rate of 100 ml min^{-1}. Information on particle size and shape was obtained with a transmission electron microscope (TEM) (JEM 2010 from JEOL) operating at 200 kV and a field-emission scanning electron microscope (FESEM) (JSM-6700F from JEOL).

Electrochemical evaluations of the catalyst performance

The catalyst performance in room temperature methanol oxidation reaction (MOR) was evaluated by cyclic voltammetry, using an Autolab PGSTAT12 potentiostat/galvanostat and a standard three-electrode cell. A catalyst ink was prepared by mixing 10 mg of catalyst with 100 μL Nafion (5 wt.% solution from Aldrich) and 900 μL ethanol.

The working electrode was a 5 mm diameter glassy carbon disk electrode cast with 10 μL catalyst ink. A Pt gauze and a Ag/AgCl (sat.) were used as the counter and the reference electrodes respectively. The potential window of 0V–1V was scanned at 20 mV s^{-1} until a stable response was obtained before the voltammograms were recorded. The electrolyte was 1 M CH_3OH in 0.5 M H_2SO_4. For the anodic stripping of CO, 10% CO in Ar was used to saturate the 0.5 M H_2SO_4 electrolyte for 30 min while the working electrode was held at –0.1 V. The passage of CO was then stopped and the electrolyte was thoroughly purged with high purity Ar. CO stripping voltammetry then commenced in the potential window of –0.18 V to 1 V starting from –0.1 V.

Results and discussion

Figure 1 shows the nitrogen adsorption–desorption isotherm and the BJH-PSD curve (inset) of MC. The isotherm displays type-IV adsorption behavior with a H2 hysteresis loop characteristic of the mesoporous materials. The BJH-PSD (inset) is centered at 3.6 nm and the surface area and pore volume were determined to be 678 $m^2\ g^{-1}$ and 0.78 $cm^3\ g^{-1}$, respectively.

Typical TEM images of the synthesized MC and Pt sol are shown in Fig. 2. Figure 2a shows a pore structure consisting of well-aligned carbon nanorods and pore size of 3.7 nm. The diameter of the carbon nanorods was estimated to be about 7 nm. Fig. 2b shows that the Pt nanoparticles in the sol had an average diameter of 4.3 nm (σ = 0.9 nm), and were lightly agglomerated despite electrostatic stabilization by the adsorbed citrate ions. The ratio

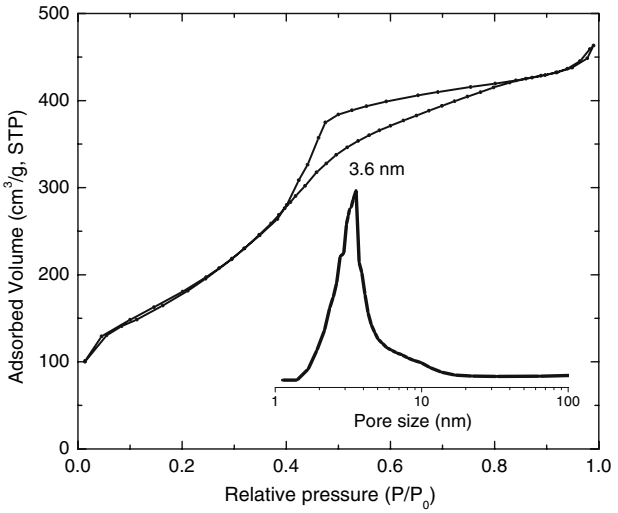

Fig. 1 Nitrogen adsorption–desorption isotherm and BJH-PSD curve (inset) of the MC

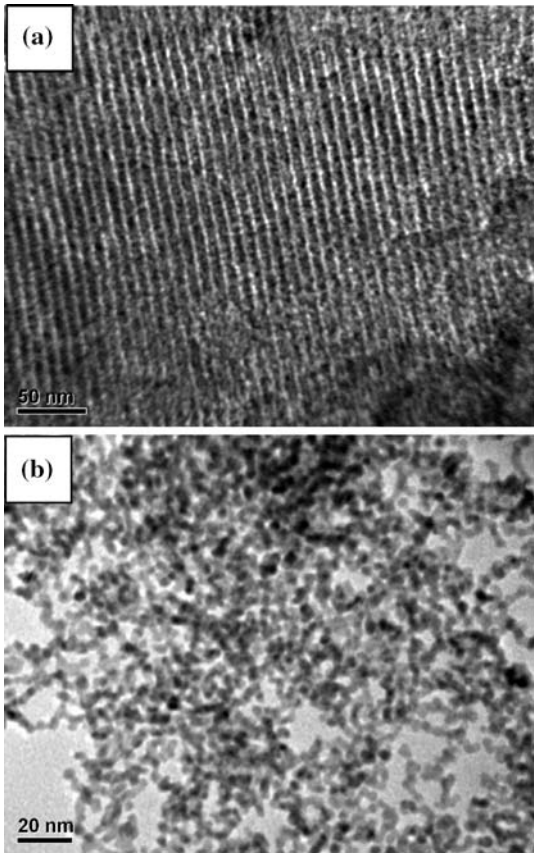

Fig. 2 TEM images of (**a**) the mesoporous carbon and (**b**) Pt colloids

of sodium citrate to Pt precursor was kept at 2:1 in the preparations of both Pt-coll/MC and Pt-impreg/MC to maximize the electrochemically active surface areas (ECSAs) and catalytic activities [12].

Typical FESEM images of MC and Pt-coll/MC (at two different magnification levels) are given in Fig. 3. Figure 3a is a low magnification image showing the overall morphology of the MC. Figure 3b focuses on the rather rough exterior of a typical MC carbon particle which should promote the attachment of adsorbed metal nanoparticles. The μm-sized MC support decorated with deposited Pt nanoparticles is shown in Fig. 3c, d. It is evident that the MC support was able to keep the Pt nanoparticles in high dispersion and well separated, quite unlike the case of the Pt sol without the MC support (Fig. 1b). The FESEM images of Pt-impreg/MC catalysts are very similar to those of Pt-coll/MC and are therefore not shown.

Figure 4 shows the thermogravimetric curves of the as-synthesized MC, and the Pt-coll/MC and Pt-impreg/MC catalysts. The SBA-15 template had been completely removed by the aqueous HF treatment, leaving negligible residue at $T > 730$ °C for the MC sample. The weights of the catalysts remained after heating at $T > 600$ °C were

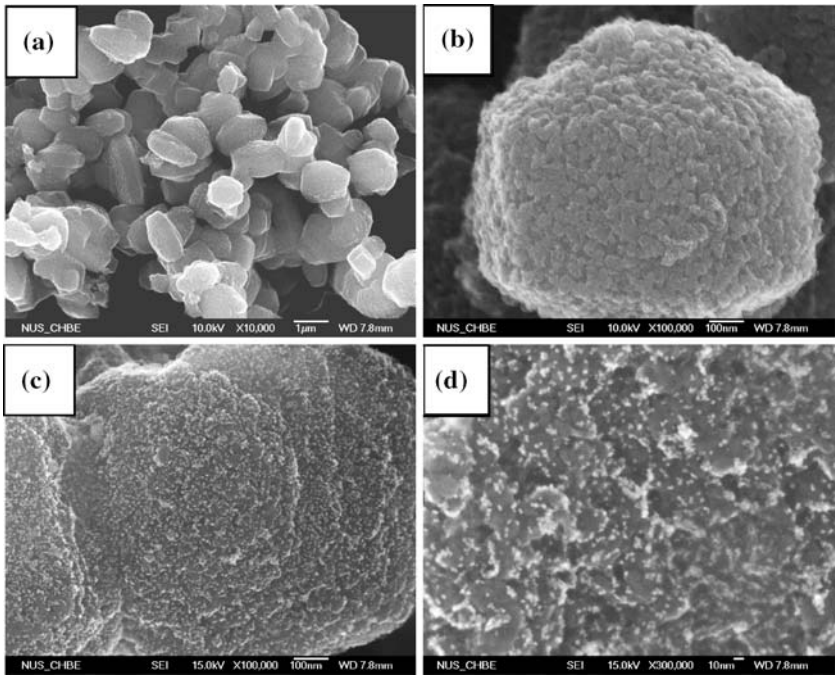

Fig. 3 FESEM images of (**a, b**) the mesoprous carbon and (**c, d**) Pt-coll/MC catalyst

assigned to Pt and were used to calculate the Pt loadings in the catalysts, which were 12 wt.% for Pt-coll/MC and 20 wt.% for Pt-impreg/MC respectively. The combustion of carbon in both the catalysts began at 200 °C, much earlier than in the case of MC alone. The sharpest decline in weight occurred at around 400 °C for the catalysts and at 600 °C for the unladen MC. This is probably due to the catalytic effect of Pt on carbon combustion.

It should be noted that the Pt loadings in both catalysts were designed to be the same, at 20 wt.%, assuming complete reduction of the Pt precursor. While the Pt loading in Pt-impreg/MC agrees well with the designed value, the 12 wt.% Pt loading in Pt-coll/MC is an obvious deviation from the target. This can be understood as follows: In the preparation of the Pt-coll/MC catalyst, Pt nanoparticles were formed first and then harvested by the carbon support. The preformed Pt nanoparticles would adsorb mostly on the carbon exterior surface because their size (4.3 nm) excluded them from entering the pores of the MC (3.6 nm). The adsorption of Pt nanoparticles on the MC exterior surface would eventually reach saturation, and the un-adsorbed nanoparticles were removed together with the filtrate, resulting in a Pt loading (12 wt.%) lower than the Pt nanoparticles produced (20 wt.%). The situation was significantly different in the preparation of the Pt-impreg/MC catalyst. There the MC support was first equilibrated with the H_2PtCl_6 solution. The dissolved metal ions, i.e. $PtCl_6^{2-}$, because of their small size, could easily penetrate the MC pores and be reduced by $NaBH_4$ upon contact. Since $NaBH_4$ reduction would lead to pore mouth plugging, the small Pt nanoparticles that were formed in the pores were ''lost'' when entrapment occurred [10]. Since the Pt nanoparticles in both cases were almost of the same size, if it is assumed that 12 wt.% represents the saturation of Pt nanoparticle adsorption on the MC exterior surface, a considerable number of Pt nanoparticles (20–12 wt.% = 8 wt.%, or 40% of the loading) could have been lost to the plugged pores. These findings support a previous work where colloid-modified Vulcan carbon supporting 2 nm Pt particles was found to saturate at a loading of 9–10 wt.% compared to that of Pt-impregnated Vulcan carbon (up to 40 wt.%). A 50% Pt

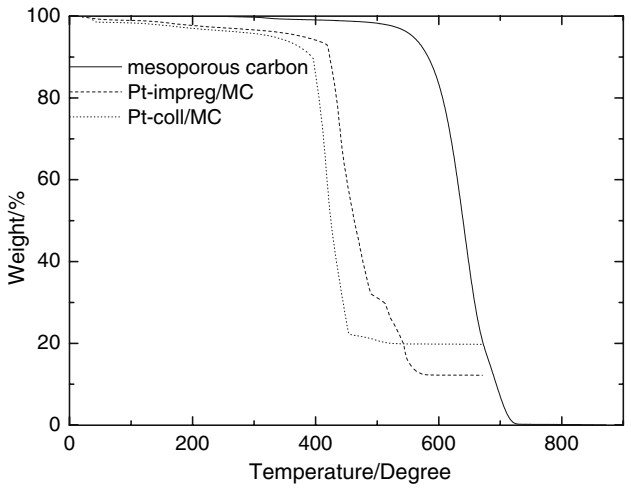

Fig. 4 Thermogravimetric behaviours of the synthesized mesoporous carbon and catalysts Pt-coll/MC and Pt-impreg/MC

entrapment in the micropores of Vulcan carbon was implicated in that work, although not directly proven [7].

The powder XRD patterns of the catalysts are shown in Fig. 5. The peak at 25° shows the graphitic nature of the MC support [13]. For both catalysts the strong diffraction peaks at Bragg angles of 39.8°, 46.2°, 67.5° and 81.3° are characteristics of face centred cubic platinum [14].

Using the Scherrer equation, the volume-averaged diameters of Pt particles in the two catalysts as determined from the line broadening of the Pt (220) peak after background subtraction [15, 16] were 4.4 nm for Pt-coll/MC and 4.1 nm for Pt-impreg/MC respectively.

The cyclic voltammograms (CV) for the supported Pt catalysts, the MC support and a glassy carbon substrate in 0.5 M H_2SO_4 are shown in Fig. 6. Within the potential range of -0.18 V to 1 V, the glassy carbon substrate had negligible current response while the MC support generated considerable capacitive charges. The redox couple (0.4 V in the forward scan and 0.26 V in the backward scan) in the CV of MC and the catalysts could arise from remnant quinine-like surface species on the carbon support [3]. For the supported Pt catalysts, the additional peak in the reverse scan at 0.55 V belonged most likely to Pt oxide reduction. The peak potential was the same for the two catalysts indicating that the Pt particles on the carbon support had similar physiochemical attributes (size and composition) [17, 18], validating the FESEM and XRD measurements. The voltammetric features in the hydrogen adsorption/desorption region on the Pt catalysts were masked by the capacitive charging from the MC support [4]. Consequently the calculation of electrochemically active surface areas, which is often carried out by integrating the well-resolved peaks in the hydrogen adsorption region, was not attempted.

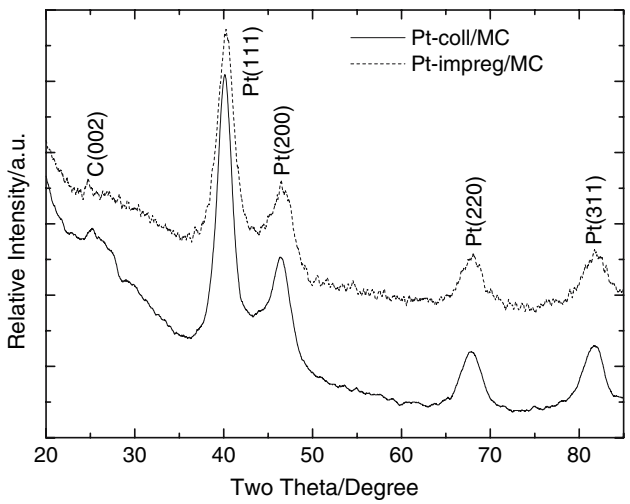

Fig. 5 XRD patterns of catalysts Pt-coll//MC and Pt-impreg/MC

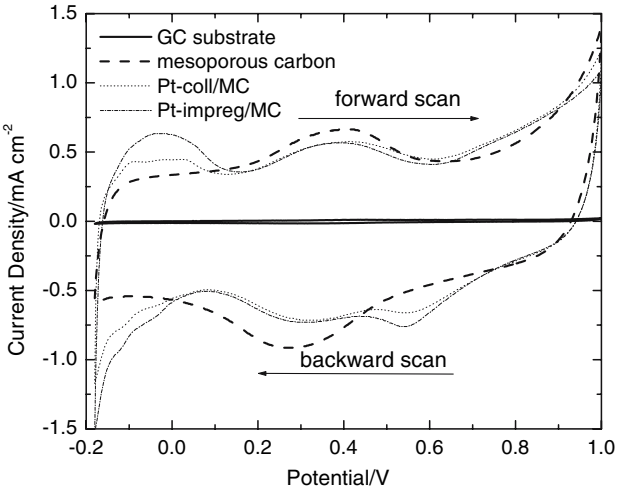

Fig. 6 Cyclic voltammograms measured at a scan rate of 20 mV s^{-1} in 0.5 M H_2SO_4 electrolyte

The CO stripping voltammograms for the Pt catalysts are compared in Fig. 7. In general the voltammetric features of CO stripping are in agreement with the literature [19]. CO oxidation went to completion in the first scan without any trace of CO in the second scan. The CO stripping voltammogram of Pt-impreg/C had an asymmetric shape with a peak at 0.62 V and a voltage plateau at 0.69 V. On the contrary, the CO stripping peak of Pt-coll/MC at about 0.56 V was symmetric, and shifted negatively compared to Pt-impreg/MC, an indication of more facile CO removal and potentially improved CO tolerance in practice. The shift in the CO anodic stripping peak could not be attributed to the particle size difference [18] since the Pt particles in both catalysts had approximately the same size. Rather the shift may have its origin in the different preparation methods. The

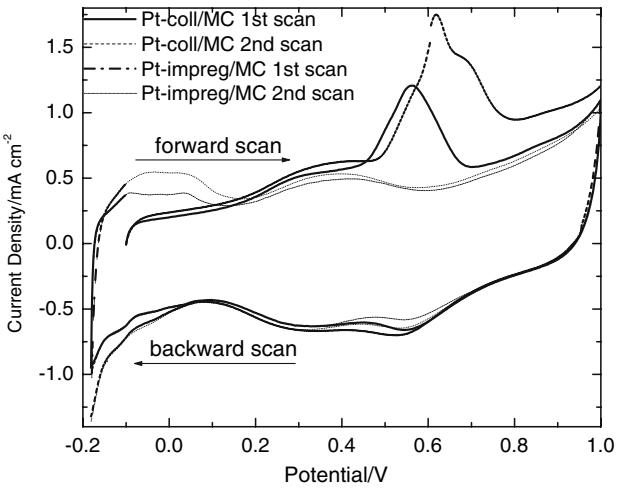

Fig. 7 Room temperature anodic CO stripping cyclic voltammograms measured at a scan rate of 20 mV s^{-1} in 0.5 M H_2SO_4 electrolyte

Pt nanoparticles in Pt-coll/MC were almost exclusively located on the external carbon exterior surface and highly accessible to the reactants. On the other hand Pt-impreg/MC had a considerable number of Pt particles located within inaccessible pores (40%). As all of the Pt nanoparticles in Pt-coll/MC were in an identical environment, CO adsorption and removal should occur to the same extent on each particle, resulting in a symmetric CO anodic stripping peak. On the contrary, CO desorption was more difficult for Pt nanoparticles in Pt-impreg/MC which were deeply seated inside the pores. The removal of CO in a constrained geometry could result in multiple desorption peaks, and the observed asymmetry in Fig. 7. It may be noted that the current density for CO oxidation was higher for Pt-impreg/MC. This is because samples had been pre-equilibrated in a static CO environment prior to the anodic stripping measurements, enabling the accessibility of all of the Pt sites in the higher loading Pt-impreg/MC.

A comparison of catalyst specific mass activities by cyclic voltammetry is shown in Fig. 8. Although the Pt loading in Pt-coll/MC (12 wt.%) was lower than that in Pt-impreg/MC (20 wt.%), the catalytic activity of Pt-coll/MC as measured by the anodic peak current density in the forward scan at around 0.69 V was marginally higher (11.1 mA cm^{-2}) than that of Pt-impreg/MC (10.0 mA cm^{-2}). If the current densities were normalized by the actual Pt loadings (12 wt.%), Pt-coll/MC would deliver 182 mA mg^{-1} Pt compared to 98 mA mg^{-1} Pt for Pt-impreg/MC. This is because the Pt sites within the pores of Pt-impreg/MC were not as accessible under the dynamical conditions of chemical reactions. Since both catalysts had about the same amount of Pt on the exterior surface of the MC support, they exhibited almost the same area-normalized activities (11.1 mA cm^{-2} vs. 10.0 mA cm^{-2}).

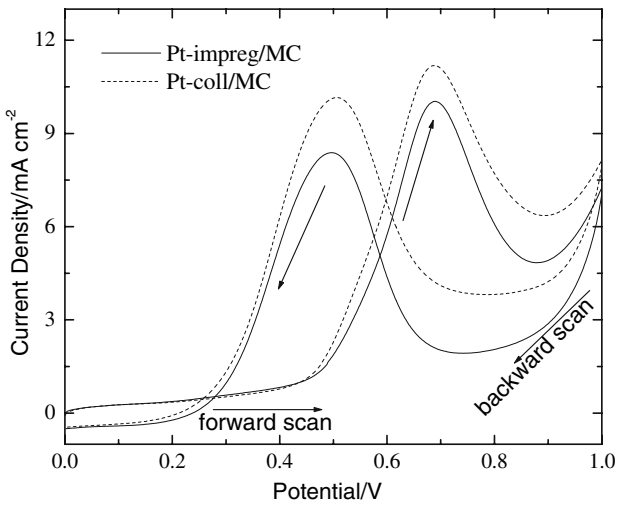

Fig. 8 Mass-normalized catalyst activities for methanol oxidation reaction in 1 M CH_3OH + 0.5 M H_2SO_4 at room temperature (scan rate = 20 mV s^{-1})

Methanol electrooxidation on the catalyst surface involves a number of simultaneous transport processes at the reaction sites: the in-diffusion of fuel molecules and the out-diffusion of the reaction products have to occur concurrently with the movement of electrons and protons via the electron conducing carbon and the proton conducting polymer (Nafion) phase respectively [9]. The transport of fuel molecules and reaction products within the mesopores (mostly 3.6 nm) is more hindered than in the open medium [8]. The overall results are one of lower CO tolerance and lower catalyst activity for Pt-impreg/MC relative to Pt-coll/MC.

Conclusions

Supported Pt catalysts were prepared by wet impregnation (Pt-impreg/MC) and by colloidal deposition (Pt-coll/MC) on template-synthesized mesoporous carbon support. Thermogravimetric analysis showed that the Pt loading in Pt-impreg/MC (20 wt.%) was in agreement with the designed value (20 wt.%) whereas the Pt loading in Pt-coll/MC (12 wt.%) was much lower. This is because Pt nanoparticles in the Pt sol that had not been adsorbed on the MC exterior surface were removed together with the filtrate during preparation. It is important to emphasize that the objective of this study is not to optimize the Pt loading for maximum metal utilization, but rather to illustrate a method of preparation which can reduce the loss of the precious metal to the micropores. The higher Pt loading in Pt-impreg/MC did not result in correspondingly higher methanol oxidation activity and CO tolerance as measured by anodic stripping voltammetry. It is hypothesized that Pt in the deep recesses of the pores was not accessible under the dynamical conditions of chemical reactions. The transport of reactants and products was also hindered in the mesopores. It is therefore concluded that the colloidal deposition method of catalyst preparation is more suitable for carbon support with a mesoporous structure. In particular the Pt particles must be larger than the pore openings to avoid the matrix entrapment effect, and hence the loss of use.

Acknowledgements The experimental work has been completed in the National University of Singapore and the authors acknowledge the research scholarship from the University.

References

1. Su F, Zeng JH, Bao XY, Yu YS, Lee JY, Zhao XS (2005) Chem Mater 17:3960
2. Su F, Zeng JH, Yu YS, Lv L, Lee JY, Zhao XS (2005) Carbon 43:2366
3. Maruyama J, Sumino K, Kawaguchi M, Abe I (2004) Carbon 42:3115

4. Ding J, Chan KY, Ren JW, Xiao F (2005) Electrochim Acta 50:3131
5. Chai GS, Shin IS, Yu JS (2004) Adv Mater 16:2057
6. Su F, Zhao XS, Wang Y, Zeng JH, Zhou ZC, Lee JY (2005) J Phys Chem B 109:20200
7. Anderson ML, Stroud RM, Rolison DR (2002) Nano Lett 2:235
8. Rolison DR (2003) Science 299:1698
9. Zeng JH, Su F, Lee JY, Zhou WJ, Zhao XS (2006) Carbon 44:1713
10. Chan KY, Ding J, Ren J, Cheng S, Tsang KY (2004) J Mater Chem 14:505
11. Lee SA, Park KW, Choi JH, Kwon BK, Sung YE (2002) J Electrochem Soc 149:A1299
12. Guo JW, Zhao TS, Prabhuram J, Wong CW (2005) Electrochim Acta 50:1973
13. Xiong L, Kannan AM, Manthiram A (2002) Electrochem Commun 4:898
14. Teng X, Yang H (2003) J Am Chem Soc 125:14559
15. Shen PK, Tian Z (2004) Electrochim Acta 49:3107
16. Li W, Zhou W, Li H, Zhou Z, Zhou B, Sun G, et al (2004) Electrochim Acta 49:1045
17. Frelink T, Visscher W, van Veen JAR (1995) J Electroanal Chem 382:65
18. Maillard F, Eikerling M, Cherstiouk OV, Schreier S, Savinova E, Stimming U (2004) Faraday Discuss 125:357
19. Papageorgopoulos DC, Keijzer M, de Bruijn FA (2002) Electrochim Acta 48:197